ELSEVIER

Journal of Alloys and Compounds 275–277 (1998) 498–504

Journal of ALLOYS AND COMPOUNDS

Magnetic properties of 4f-based intermetallics studied by means of ^{155}Gd Mössbauer spectroscopy

K.H.J. Buschow[a,*], F.M. Mulder[b], R.C. Thiel[c]

[a]*Van der Waals-Zeeman Institute, University of Amsterdam, Valckenierstraat 65, 1018 XE Amsterdam, The Netherlands*
[b]*I.R.I., Technical University of Delft, Mekelweg 15, 2629 JB Delft, The Netherlands*
[c]*Kamerlingh Onnes Laboratory, University of Leiden, Nieuwsteeg 18, 2300 RA Leiden, The Netherlands*

Abstract

In this report the possibilities to obtain experimental information on various physical properties of rare earth intermetallics by means of ^{155}Gd Mössbauer spectroscopy are reviewed. Results are discussed of compounds related to permanent magnet materials, hydrogen absorbing materials, superconducting and heavy-electron systems. Particular attention is paid to the electric field gradient V_{zz} and its relation to the second order crystal field parameter A_2^0. Experimental data are compared with results of electronic structure calculations. © 1998 Elsevier Science S.A.

Keywords: ^{155}Gd Mössbauer spectroscopy; Electric field gradient; Second order crystal field parameter; Rare earth intermetallics

1. Introduction

The Gd nucleus is a most useful probe for studying atomic scale properties at the rare earth site in various types of intermetallic compounds. For obtaining ^{155}Gd Mössbauer spectra, generally only small amounts of powder samples are required, the measuring times being of the order of several hours. From the Zeeman splitting of the spectra information on the magnetic interaction between the localised moments can be obtained whereas the isomer shift can be employed to obtain information regarding the bonding of the rare earth atoms to the other components present in a given compound. Of considerable importance is the possibility to utilise ^{155}Gd Mössbauer spectroscopy for obtaining information on the rare earth contribution to the magnetic anisotropy.

In several previous investigations we have used the quadrupole splitting of the spectra to study the behaviour of the electric field gradient (V_{zz}) at the nuclear site in a variety of different Gd compounds. The results have subsequently been employed to obtain experimental information on the crystal field splitting, since the values of V_{zz} can be taken as a measure of the second order crystal field parameter A_2^0. In the case of complicated crystal field interactions, ^{155}Gd Mössbauer spectroscopy is most useful because it samples exclusively sign and magnitude of the second order crystal field parameter, whatever the sign and magnitude of the higher order crystal field parameters.

This report is organised as follows. In the next section we will briefly describe the experimental method used to obtain ^{155}Gd Mössbauer spectra and the procedure followed to analyze these spectra. In Section 3 we will discuss in some detail the physical origin of the electric field gradient present at the Gd nuclear site and the electric field gradient experienced by the 4f electrons. In Section 4, Section 5 and Section 6 a survey will be given of how ^{155}Gd Mössbauer spectroscopy has been successfully applied in various groups of materials to obtain information on their magnetic properties.

2. Experimental methodology

The ^{155}Gd Mössbauer spectra of the compounds described in this report were obtained by means of the 86.5 keV resonance of ^{155}Gd. The source material was prepared from neutron-irradiated $SmPd_3$ enriched to 98% in ^{154}Sm. More details of the spectrometer are described elsewhere [1]. The spectra were analyzed by means of a least-squares fitting procedure. The latter included diagonalisation of the full nuclear Hamiltonian and the employment of a transmission integral. Our independently refined hyperfine

*Corresponding author. Tel.: +31 20 5255714; fax: +31 20 5255788; e-mail: buschow@phys.uva.nl

PII: S0925-8388(98)00380-6

parameters consisted of the isomer shift IS, the effective hyperfine field H_{eff}, and the quadrupole splitting

$$QS = \tfrac{1}{4}eQV_{ZZ}(3\cos^2\theta + 1 + \eta\sin^2\theta\cos 2\phi) \quad (1)$$

where Q is the nuclear quadrupole moment ($Q = 1.30 \times 10^{-28}$ m^{-2}). The asymmetry parameter η is zero for compounds with cubic and hexagonal point symmetry. The angle θ between H_{eff} and the c axis was generally kept as an adjustable parameter, excepting those cases where experimental information of the easy magnetisation direction was available from other types of measurements. The line width of absorber and source were constrained to 0.25 and 0.36 mm/s for the transmission integral.

3. Relation between V_{ZZ} and A_2^0

Band structure calculations made for several types of rare earth intermetallics showed that the electric field gradient is primarily determined by the asphericity of the on-site valence electron charge clouds of the Gd atoms [2–5]. These results made it also clear that the commonly assumed relation of the form

$$A_2^0 = -V_{ZZ}(1-\sigma_2)/4(1-\gamma_\infty), \quad (2)$$

where σ_2 is an electronic screening factor and γ_∞ the Sternheimer antishielding factor, lacks a fundamental basis. The reason for this is that core excitations and the concomitant Sternheimer antishielding play only a minor role in determining the electric field gradient at the nuclear site [3]. The difference between A_2^0 and V_{ZZ} results from the fact that the on-site 5d electron charge cloud asphericity, determining mainly the former, and the on-site 6p charge cloud asphericity mainly responsible for the latter, need not be the same. However, strong indications exist, based on computational results [5] as well as on experimental results [7], that there is still a relation between A_2^0 and V_{ZZ}. We will investigate this point in more detail below. The main difficulty from the experimental side is the restricted availability of reliable experimental data for A_2^0. The reason for this difficulty originates from the fact that experimental methods commonly employed for the determination of A_2^0 (inelastic neutron scattering, magnetic measurements on single crystals, specific heat measurements) involve fits to the experimental data in which not only A_2^0 but also several of the higher order crystal field parameters A_n^m have to be considered simultaneously. There exist, however, data of A_2^0 that were obtained by using a combination of two or even all three of the techniques mentioned. One of the most favourable cases is the series $RGa_{2-x}Al_x$ (hexagonal, AlB_2 type) studied by means of inelastic neutron scattering, measurements of the specific heat and magnetic properties on single crystals [8,9]. The concentration-dependent change in magnitude and sign of A_2^0 in compounds of the series has been used by us in a previous investigation [7] to determine the proportionality constant ω in the semi-empirical relation

$$A_2^0[Ka_0^{-2}] = -\omega V_{ZZ}[10^{21}Vm^{-2}], \quad (3)$$

employing the fact that a similar change in sign and magnitude was found for V_{ZZ} from Gd Mössbauer spectroscopy. The empirical value found in this way is $\omega = 35$. The RNi_5 compounds (hexagonal, $CaCu_5$ type) form an almost equally favourable series for which A_2^0 values have been determined by a combination of the same three techniques [10,11]. A typical value of A_2^0 representative for most of the RNi_5 compounds is around $-450\ Ka_0^{-2}$. With the value $V_{ZZ} = 9.7 \times 10^{21}\ Vm^{-2}$ one then finds $\omega = 46$. The closeness of the two empirical values derived for ω is surprising, given the fact that these values are derived on compounds of dissimilar crystal structures in which Gd is combined with elements of an equally dissimilar nature. This encourages us to advocate future application of the empirical relation with $\omega = 40 \pm 8$. We will return to this point in the last section of this report, after having discussed ^{155}Gd Mössbauer data obtained in several interesting groups of materials.

4. Compounds related to permanent magnet materials

The 20th century has witnessed quite an extraordinary development in hard magnetic materials. Developments have been strong in the last few decades of this century, after the advent of rare earth permanent magnets (REPM) in particular. Permanent magnet materials of this type are based on intermetallic compounds of rare earths and Fe or Co. They derive their exceptional properties from the favourable combination of properties inherent in the rare earth sublattice and in the 3d sublattice, the former mainly providing the magnetic anisotropy, the latter providing a high magnetization and a high magnetic ordering temperature. There are two important prototypes of REPM. Magnets based on Sm and Co are unsurpassed with regard to their high coercivities and their low temperature coefficients of coercity and magnetization, even at temperatures far above room temperature. Magnets based on Nd, Fe and B are unequalled with regard to the maximum energy product and their comparatively low price. Mössbauer data obtained on the corresponding Gd compounds have been collected in Table 1, together with data on Gd compounds of related materials. Of particular interest are the interstitial solid solutions of compounds of the 2:17 type and 1:12 type where the filling of the interstitial holes by nitrogen or carbon is seen to lead to drastic changes of V_{ZZ}. The strong enhancement of V_{ZZ} implies an equally strong enhancement of A_2^0 and the corresponding crystal field induced rare earth sublattice

Table 1
Hyperfine parameters derived from fitting of the Gd-Mössbauer spectra of several Gd compounds related to permanent magnet materials of the same crystal structure

Compound	Structure	V_{zz}	θ	η	B_{hf}	IS	I	Ref.
$GdCo_5$	$CaCu_5$	10.1	0	—	7.4	0.24	1.0	[12]
$Gd_2Fe_{14}B$	$Nd_2Fe_{14}B$	−7.75	0	0.61	9.4	0.217	0.5	[13]
		11.37	90	0.35	20.1	0.204	0.5	
$Gd_2Co_{14}B$	$Nd_2Fe_{14}B$	−8.3	90	0.6	10.9	0.26	0.5	[14,15]
		+8.5	45	0.3	3.6	0.22	0.5	
Gd_2Fe_{17}	Th_2Zn_{17}	4.3	90	—	21	0.25	1.0	[16]
$Gd_2Fe_{17}N_x$	Th_2Zn_{17}	12.6	90	—	4.7	0.47	1.0	[16]
Gd_2Co_{17}	Th_2Zn_{17}	4.8	90	—	4.7	0.24	1.0	[5]
$Gd_2Co_{17}N_x$	Th_2Zn_{17}	14.9	0	—	10.3	0.45	1.0	[5]
$GdCo_{11}Ti$	$ThMn_{12}$	−2.3	0		13.5	0.23	1.0	[17]
$GdFe_{11.5}Mo_{1.5}$	$ThMn_{12}$	1.6	0	—	9.2	0.21	1.0	[18]
$GdFe_{11.5}Mo_{1.5}N_x$	$ThMn_{12}$	−21.3	90	—	7.2	0.35	1.0	[18]
$GdFe_9Ti_2$	$CeMn_6Ni_5$	2.6	0	—	14.7	0.22	1.0	[17]

The data are given in the following units: V_{zz} [10^{21} V/m^2], B_{hf} [T], IS [mm/s], θ [deg]. I is the relative intensity of the subspectra when there is more than one crystallographic site. All values listed for V_{zz} were obtained with the same value for the quadrupole moment Q.

anisotropy. The latter is a major prerequisite for application of these materials as permanent magnets [19].

5. Compounds related to superconducting and heavy-electron materials

Quaternary intermetallic compounds of the type RNi_2B_2C have received considerable attention recently because several of its members are superconductors with transition temperature close to 17 K [20]. The superconducting transition temperature becomes strongly lowered when R carries a magnetic moment. Because of the interesting interplay between magnetism and superconductivity in these materials reports of numerous investigations of magnetic properties [21] and rare earth Mössbauer spectroscopy [22–25] have appeared recently, including those of compounds of the type RCo_2B_2C [26]. The interpretation of the magnetic properties appears to be fairly difficult because of the presence of crystal field effects requiring the knowledge of crystal field parameters up to the sixth order. All these parameters have to be considered as variables when fitting the results of magnetisation, specific heat and neutron scattering to model descriptions.

In this case ^{155}Gd Mössbauer spectroscopy is particularly helpful because, via V_{zz}, it samples exclusively the second order term. A further favourable circumstance is the fact that the magnetic ordering temperatures are sufficiently low so that it is possible to obtain spectra in the paramagnetic regime. Because of the absence of hyperfine splitting the spectra show only quadrupole splitting (Fig. 1). In fact Eq. (1) reduces to the simple form $QS = 1/4\ eQV_{zz}$ so that the electric field gradient can be obtained from the spectra most reliably as the only adjustable parameter, avoiding all the difficulties associated with the complex magnetically ordered state [21]. Using relation (3) with $\omega = 40 \pm 8$, and the data listed for V_{zz} in Table 2 one may derive the following values: $A_2^0 = -(484 \pm 97)\ Ka_0^{-2}$ for compounds of the RNi_2B_2C series; $A_2^0 = -(296 \pm 59)\ Ka_0^{-2}$ for compounds of the RCo_2B_2C series.

Apart from the compounds related to superconducting materials we have listed in Table 2 hyperfine parameters obtained on compounds related to heavy-electron systems. Several of the Ce based compounds of similar crystal structure and composition as the Gd compounds listed in the table display such heavy electron behaviour (see for instance Ref. [30] and papers cited therein). Also for these compounds it is important to have information on the crystal field level splitting and on how the level splitting can vary across a series of isotypic compounds.

However, in some cases the A_2^0 value of the Ce compounds may deviate from that for other rare earth compounds of the same series. This can be easily explained when account is taken of the fact that A_2^0 is determined primarily by the 5d electron charge asphericities, because in Ce compounds there may be some mixing of 5d electron states with 4f electron states, which can substantially affect the 5d electron charge cloud asphericities.

Frequently it is tacitly assumed that the crystal field parameters do not vary much across a series of isotypic compounds in which the transition metal component is varied. The results listed for two representatives of the RT_2Si_2 series show clearly that this is a misconception, because V_{zz} (and A_2^0) vary appreciably when passing across the 5d series from T = Ru to T = Ag, and even give rise to a sign reversal (see Fig. 2a). Results of electronic band structure calculations have confirmed this picture and provided a physical explanation for the occurrence of the sign reversal [2].

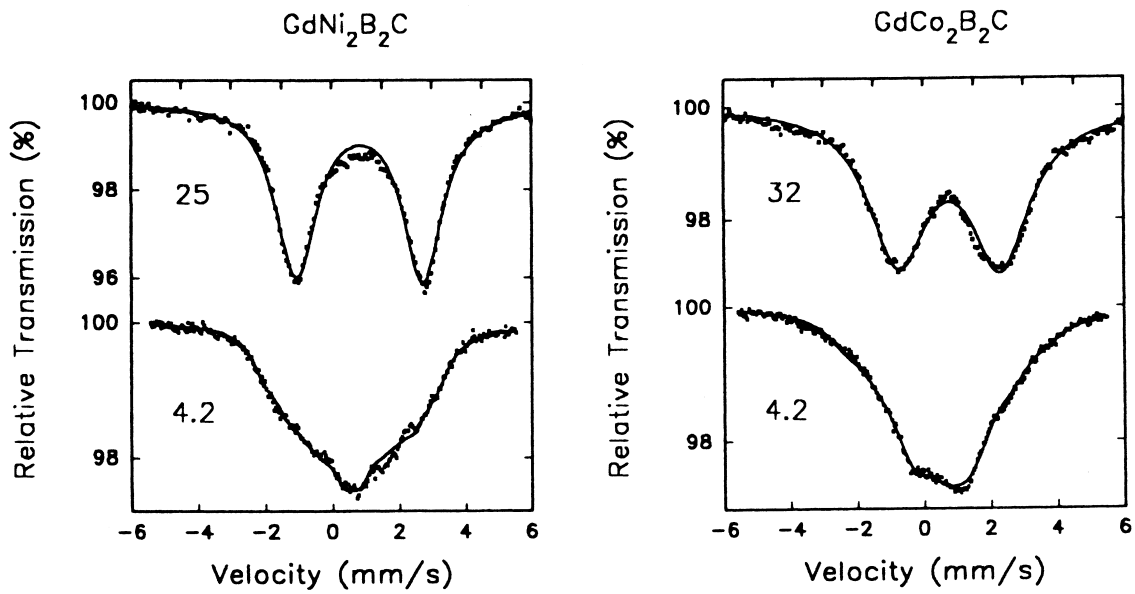

Fig. 1. ^{155}Gd Mössbauer spectra of $GdNi_2B_2C$ and $GdCo_2B_2C$ obtained at the temperatures indicated in the figure. The spectra shown in the top parts were obtained in the paramagnetic state and show quadrupole splitting only.

6. Metal hydrides

A realistic description of the state of hydrogen in metallic systems is difficult and many experimental efforts have been spent to decide between the so-called hydridic or anionic model and the protonic model. In the hydridic model the two 1s electron states of the hydrogen are located below the Fermi energy of the metal. In the hydride both these two levels are occupied. The extra electron is provided by the conduction band and the hydrogen is present as H^-. By contrast, the two 1s electron states of hydrogen are situated above the Fermi level in the protonic model. In that case the hydrogen donates one electron to the conduction band upon hydride formation and is present as H^+. The difficulties associated with both model descriptions are due to the fact that some experimental results favour the anionic model while other experimental results are more conveniently interpreted in terms of the protonic model.

The possibility to perform modern electronic band structure calculations for a large number of metallic hydrides have removed much of the controversy between the two models. Such calculations have shown that the hydrogen in the hydride has to be regarded as a proton screened by variable amounts of valence electrons. A comprehensive description of the results of electronic band structure calculations can be found in the reviews written by Schlapbach et al. [31] and Yamaguchi and Akiba [32]. In these reviews one may also find a description of the changes in physical properties upon hydrogen absorption, including magnetic and electrical transport properties.

Here we will mention briefly a few examples of investigations made by means of ^{155}Gd Mössbauer spectroscopy on ternary hydrides. We have chosen investigations made on several compounds of the composition GdM_2, where M = Ru, Rh and Cu [33–35]. The changes in isomer shift of Gd have been described in detail by de Vries et al. [36] in terms of volume contraction upon compound formation and charge transfer. When concentrating on the effect of the hydrogen absorption, one finds that it leads to fairly strong increases in isomer shift. This increase is consistent with a reduction in s electron density at the Gd nuclei, indicating charge transfer in the direction Gd→H. Simultaneously, a strong increase in the absolute value of the hyperfine field is seen to take place (Fig. 2b). Hyperfine fields at the Gd nucleus are commonly inter-

Table 2
Hyperfine parameters derived from fitting of the Gd-Mössbauer spectra of several Gd compounds related to superconducting and heavy-electron materials of the same crystal structure

Compound	Structure	V_{zz}	θ	$\lvert B_{hf}\rvert$	IS	I	Ref.
$GdNi_2B_2C$	YNi_2B_2C	11.9	56	27.9	0.56	1.0	[26]
$GdCo_2B_2C$	YNi_2B_2C	9.6	44	45.6	0.50	1.0	[26]
$GdPd_2Al_3$	$PrNi_2Al_3$	+12.6	49	26.0	0.48	0.81	[27]
$GdCu_5$	$CaCu_5$	+9.1	47	23.2	0.25	1.0	[28]
$GdCo_3B_2$	$CeCo_3B_2$	+31.9	90	15.0	0.20	1.0	[12]
$GdRu_2Si_2$	$ThCr_2Si_2$	−18.5	50	29.2	0.43	1.0	[29]
$GdAg_2Si_2$	$ThCr_2Si_2$	+4.3	90	27.2	0.67	1.0	[29]

The data are given in the following units: V_{zz} [10^{21} V/m^2], B_{hf} [T], IS [mm/s], θ [deg]. I is the relative intensity of the subspectra. In the case of $GdPd_2Al_3$ there is a small degree of Pd-Al site disorder, causing a distribution of subspectra. Only the data for the main subspectrum have been listed for this compound.

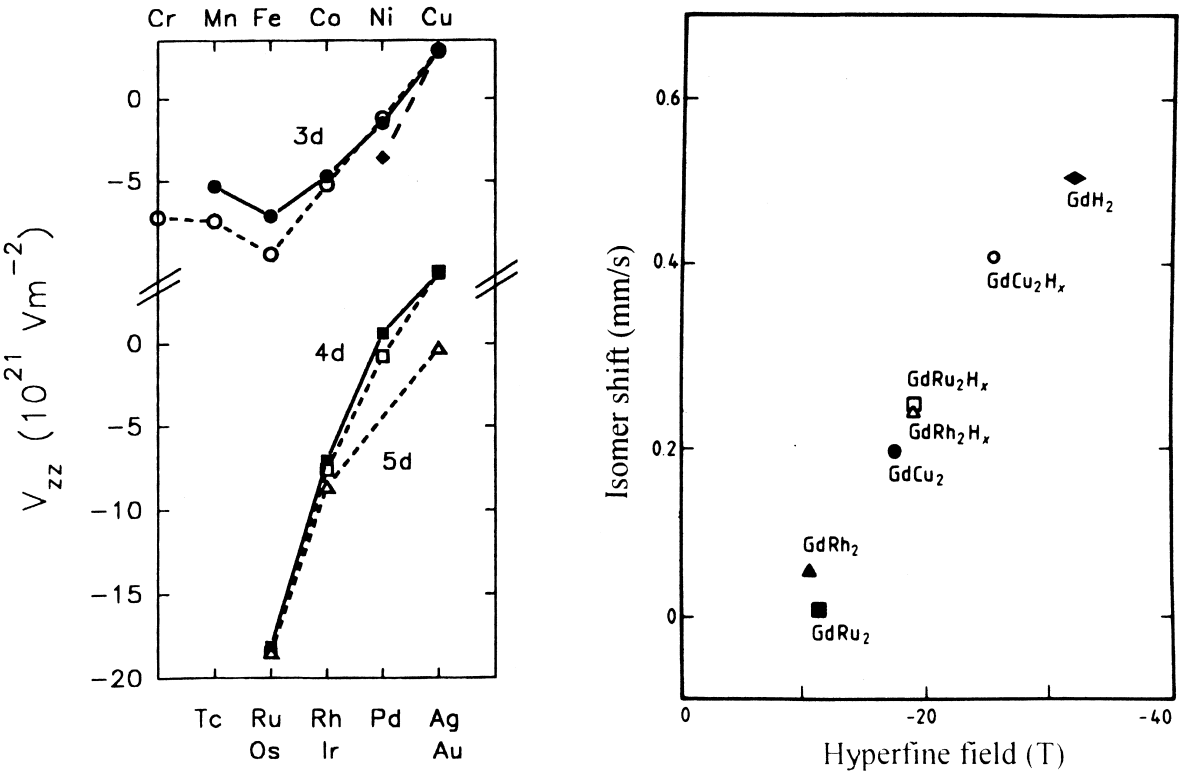

Fig. 2. Left: values of V_{zz} of various GdT_2X_2 compounds plotted vs. the atomic number of the transition metal component T. Full symbols GdT_2Ge_2 and GdT_2Sb_2; open symbols GdT_2Si_2. Circles represent compounds in which T is a 3d element; squares 4d, triangles 5d. Full diamonds: GdT_2Sb_2. Right: plot of hyperfine field vs. isomer shift for various compounds of the type (GdM_2 M=Ru, Rh and Cu) and the corresponding hydrides.

preted as arising from a negative core contribution (−33.4 T) and a positive conduction electron contribution. The increase in absolute value of the hyperfine field displayed in the figure reflects a decreasing conduction electron contribution, culminating in the result shown for GdH_2 [35], which is a semiconductor when present in slightly off-stoichiometric form.

7. Comparison with calculational results

For several of the compounds discussed, electronic band structure calculations have become available, which allows a comparison of the hyperfine parameters derived from Mössbauer spectroscopy with those calculated.

Some difficulties exist with respect to the hyperfine fields. As may be seen from Table 1 the hyperfine field values fall into a fairly wide range. Although the relative differences in hyperfine fields can adequately be explained by theory, the calculated and experimental hyperfine fields differ systematically by an overall shift of 25 T [37]. This discrepancy seems to be independent of the type of approximation used for the calculations [37,39], and its origin is still unclear.

Computational and experimental results of V_{ZZ} and A_2^0 for a restricted group of materials can be compared in Table 3. In general, the agreement between experimental values of V_{ZZ} and theory can be said to be satisfactory. As to A_2^0, there is a lack of reliable experimental data. Fortunately, the A_2^0 values reported in the literature for the RNi_5 compounds and the $R_2Fe_{14}B$ compounds do not vary much within the corresponding lanthanide series [9,10,42], which lends credence to the reliability of the A_2^0 data. The situation is different for the RCo_5 where the A_2^0 values vary strongly within the series [11]. The value of A_2^0 listed in the table is based on the values reported for $NdCo_5$ and $HoCo_5$. These values were chosen because they are almost equal to each other and refer to a light and heavy rare earth element, respectively. Disregarding the lack of experimental A_2^0 data for the moment, it is interesting to note that different types of electronic structure calculations do not lead to the same answer. Surprisingly, however, the corresponding calculated values of the ratio $\omega = -A_2^0/V_{ZZ}$ are rather close to each other. Inspection of the data listed in the table furthermore shows that the calculated ω ratios are also close to the experimental ω ratios. This can be taken as support for the applicability of relation (2).

8. Concluding remarks

In this report we have presented examples of investigations where important experimental information on various physical quantities was obtained by means of

Table 3
Experimental values of hyperfine parameters [exp] derived from fitting of the Gd-Mössbauer spectra of several Gd compounds in comparison with results derived from band structure calculations [cal]

Compound	V_{zz}[cal]	V_{zz}[exp]	A_2^0[cal]	A_2^0[exp]	ω[cal]	ω[exp]
$GdNi_5$	+16.2 [3]	+9.7 [3]		−450 [10]		46
$GdCo_5$	+14.0 [3]	+10.1 [3]	−691 [40]	−400 [11]	49 [3,40]	40
	+18.3 [6]		−972 [6]		53 [6]	
	+10.8 [38]		−584 [38]		54 [38]	
Gd_2Co_{17}	+6.8 [5]	+4.8 [5]	−169 [4]			35
Gd_2Fe_{17}	+7.5 [4]	+4.3 [16]	−302 [40]		40 [4,40]	
	+4.8 [39]					
	+6.4 [41]		−302 [41]		47 [41]	
$Gd_2Fe_{17}N_x$	+10.5 [41]	+12.6 [5]	−475 [41]		45 [41]	
	+11.0 [39]					
$Gd_2Fe_{17}C_x$	+13.8 [41]	+15 [42]	−613 [41]		44 [41]	
	+14.9 [39]					
$Gd_2Co_{17}N_x$	+14.8 [5]	+14.9 [5]				
$Gd_2Fe_{14}B$(f)	−8.8 [4]	−7.75 [13]	+371 [4]	+300 [42]	42 [4]	39
$Gd_2Fe_{14}B$(g)	−7.7 [4]	−7.67[a] [13]	+381 [4]	+300 [42]	49 [4]	39
$GdNi_2B_2C$	+12.8 [26]	+11.9 [26]		−379 [43]		32

The data are given in the following units: V_{zz} [10^{21} V/m^2], A_2^0 [Ka_0^{-2}].
[a]Component of the electric field gradient in the *c* direction.

^{155}Gd Mössbauer spectroscopy. This technique allows for a fast and unambiguous characterisation of the electric field gradient using the empirical relationship in Section 3. ^{155}Gd Mössbauer spectroscopy provides a local probe which is complementary to results that may be obtained from inelastic neutron scattering.

References

[1] H. de Graaf, Thesis, University of Leiden, 1982.
[2] R. Coehoorn, K.H.J. Buschow, M.W. Dirken, R.C. Thiel, Phys. Rev. B 42 (1990) 4645.
[3] K.H.J. Buschow, R. Coehoorn, F.M. Mulder, R.C. Thiel, J. Magn. Magn. Mater. 118 (1993) 347.
[4] R. Coehoorn, K.H.J. Buschow, J. Appl. Phys. 69 (1991) 5590.
[5] F.M. Mulder, R.C. Thiel, R. Coehoorn, T.H. Jacobs, K.H.J. Buschow, J. Magn. Magn. Mater. 117 (1992) 413.
[6] G.H.O. Daalderop, P.J. Kelly, M.F.H. Schuurmans, Phys. Rev. B 53 (1996) 14415.
[7] F.M. Mulder, R.C. Thiel, K.H.J. Buschow, J. Alloys Comp. 203 (1994) 97.
[8] F.Y. Zhang, Thesis, University Joseph Fourier, Grenoble, 1992.
[9] D. Gignoux, D. Schmitt, in: K.H.J. Buschow (Ed.), Handbook of Magnetic Materials, vol. 10, North Holland, Amsterdam 1997, p. 239.
[10] F.E. Kayzel, Thesis, University Amsterdam, Amsterdam 1997.
[11] J.J.M. Franse, R.J. Radwanski, in: K.H.J. Buschow (Ed.), Handbook of Magnetic Materials, vol. 7, North Holland, Amsterdam, 1993, p. 307.
[12] H.H.A. Smit, R.C. Thiel, K.H.J. Buschow, J. Phys. F 18 (1988) 295.
[13] M. Bogé, C. Czjzek, D. Givord, C. Jeandry, H.S. Li, J.L. Oddou, J. Phys. F 16 (1986) L67.
[14] H.H.A. Smit, R.C. Thiel, K.H.J. Buschow, Physica B 145 (1987) 329.
[15] H. Yamauchi, H. Yamamoto, H. Hirosawa, M. Sagawa, J. Magn. Magn. Mater. 70 (1987) 340.
[16] M.W. Dirken, R.C. Thiel, R. Coehoorn, T.H. Jacobs, K.H.J. Buschow, J. Magn. Magn. Mater. 94 (1991) L15.
[17] F.M. Mulder, R.C. Thiel, L.D. Tung, J.J.M. Franse, K.H.J. Buschow, J. Alloys Comp. 264 (1998) 43.
[18] D.P. Middleton, D.A. van Straat, F.M. Mulder, R.C. Thiel, K.H.J. Buschow, J. Appl. Phys. 79 (1996) 4593.
[19] H. Fujii, H. Sun, in: K.H.J. Buschow (Ed.), Handbook of Magnetic Materials, vol. 9, North Holland, Amsterdam, 1995, p. 303.
[20] R.J. Cava, H. Takagi, H.W. Zandbergen, J.J. Krajewski, W.F. Peck, T. Siegrist, B. Batlogg, R.B. van Dover, R.J. Felder, K. Mizuhashi, J.O. Lee, H. Eisaki, S. Ushida, Nature 367 (1994) 252.
[21] J.W. Lynn, S. Skanthakumar, Q. Huang, S.K. Sinha, Z. Hossain, L.C. Gupta, R. Nagarajan, C. Godart, Phys. Rev. B 55 (1997) 6584.
[22] P. Bonville, J.A. Hodges, C. Vaast, E. Alleno, C. Godart, L.C. Gupta, Z. Hossain, R. Nagarajan, G. Hilscher, H. Michor, Z. Phys. B 101 (1996) 520.
[23] J.P. Sanchez, P. Vulliet, C. Godart, L.C. Gupta, Z. Hossain, R. Nagarajan, Phys. Rev. B 54 (1996) 9421.
[24] A.M. Mulders, P.C.M. Gubbens, U. Gasser, C. Baines, K.H.J. Buschow, Phys. Rev. B (1997).
[25] A.M. Mulders, P.C.M. Gubbens, K.H.J. Buschow, Phys. Rev. B 54 (1996) 14963.
[26] F.M. Mulder, J.H.V.J. Brabers, R. Coehoorn, R.C. Thiel, K.H.J. Buschow, F.R. de Boer, J. Alloys Comp. 217 (1995) 118.
[27] F.M. Mulder, R.C. Thiel, K.H.J. Buschow, J. Alloys Comp. 223 (1995) 127.
[28] F.M. Mulder, R.C. Thiel, K.H.J. Buschow, J. Alloys Comp. 190 (1992) 77.
[29] M.W. Dirken, R.C. Thiel, K.H.J. Buschow, J. Less-Common Met. 146 (1989) 147.
[30] G.J. Nieuwenhuys, in: K.H.J. Buschow (Ed.), Handbook of Magnetic Materials, vol. 9, North Holland, Amsterdam, 1995, p. 1.
[31] L. Schlapbach, I. Anderson, J.P. Burger, in: Materials Science and Technology, vol. 3B, VCH Verlag, Weinheim, 1994, p. 270.
[32] M. Yamaguchi, E. Akiba, in: Materials Science and Technology, vol. 3B, VCH Verlag, Weinheim, 1994, p. 399.
[33] H. de Graaf, R.C. Thiel, K.H.J. Buschow, J. Phys. F 12 (1982) 1239.
[34] I. Jacob, E.R. Bauminger, D. Davidov, I. Felner, S. Ofer, D. Shaltiel, J. Magn. Magn. Mater. 15–18 (1980) 1269.
[35] J.D. Cashion, D.B. Prowse, A. Vas, J. Phys. C 6 (1973) 2611.
[36] J.W.C. de Vries, R.C. Thiel, K.H.J. Buschow, J. Phys. F 15 (1985) 2403.

[37] R. Coehoorn, K.H.J. Buschow, J. Magn. Magn. Mater. 118 (1993) 175.
[38] K. Hummler, M. Fähnle, Phys. Rev. B 53 (1996) 3272.
[39] P. Uebele, K. Hummler, M. Fähnle, Phys. Rev. B 53 (1996) 3296.
[40] R. Coehoorn, in: D.G. Pettifor, A.H. Cottrell (Eds.), Electron Theory in Alloy Design, The Institute of Materials, 1992.
[41] R. Coehoorn, G.H.O. Daalderop, J. Magn. Magn. Mater. 104–107 (1992) 1081.
[42] K.H.J. Buschow, Rep. Prog. Phys. 54 (1991) 1123.
[43] J.S. Gardner, C.V. Tomy, L. Afalfiz, G. Balakrishnan, D. McK Paul, B.D. Rainford, R. Cywinski, R.S. Eccleston, E.A. Goremychkin, Physica B 213–214 (1995) 136.